



Ingeniería, investigación y tecnología

ISSN: 1405-7743

Universidad Nacional Autónoma de México, Facultad de Ingeniería

Yáñez-Valdez, Ricardo; Luna-Díaz, Ángel Iván; Cos-Díaz, Jorge  
Jayr; Cuenca-Jiménez, Francisco; Velázquez-Villegas, Fernando  
Structural dynamics of a 3 DOF parallel kinematic machine  
Ingeniería, investigación y tecnología, vol. XXII, no. 2, 2021, -June, pp. 1-13  
Universidad Nacional Autónoma de México, Facultad de Ingeniería

DOI: <https://doi.org/10.22201/fi.25940732e.2021.22.2.013>

Available in: <https://www.redalyc.org/articulo.oa?id=40471796005>

- How to cite
- Complete issue
- More information about this article
- Journal's webpage in redalyc.org

redalyc.org

Scientific Information System Redalyc

Network of Scientific Journals from Latin America and the Caribbean, Spain and Portugal

Project academic non-profit, developed under the open access initiative



## Structural dynamics of a 3 DOF parallel kinematic machine

## Dinámica estructural de una máquina herramienta de configuración paralela de 3 GDL

Yáñez-Valdez Ricardo

Universidad Nacional Autónoma de México

Facultad de ingeniería

Departamento de Ingeniería de Diseño y Manufactura

E-mail: [ryv77@unam.mx](mailto:ryv77@unam.mx)

<https://orcid.org/0000-0002-8518-0906>

Luna-Díaz Ángel Iván

Universidad Nacional Autónoma de México

Facultad de ingeniería

Departamento de Ingeniería de Diseño y Manufactura

E-mail: [ivanpuma06@hotmail.com](mailto:ivanpuma06@hotmail.com)

<https://orcid.org/0000-0002-5171-9037>

Cos-Díaz Jorge Jayr

Universidad Nacional Autónoma de México

Facultad de ingeniería

Departamento de Ingeniería de Diseño y Manufactura

E-mail: [icosdi@gmail.com](mailto:icosdi@gmail.com)

<https://orcid.org/0000-0002-8955-459X>

Cuenca-Jiménez Francisco

Universidad Nacional Autónoma de México

Facultad de ingeniería

Departamento de Ingeniería de Diseño y Manufactura

E-mail: [fracuenc@comunidad.unam.mx](mailto:fracuenc@comunidad.unam.mx)

<https://orcid.org/0000-0002-8372-464X>

Velázquez-Villegas Fernando

Universidad Nacional Autónoma de México

Facultad de ingeniería

Departamento de Ingeniería de Diseño y Manufactura

E-mail: [fernvel@unam.mx](mailto:fernvel@unam.mx)

<https://orcid.org/0000-0002-3199-420X>

### Abstract

Milling is an intrinsically interrupted cutting operation; therefore, vibrations occur. There are both self-excited (chatter) and forced vibration. Vibrations in milling appear due to the lack of dynamic stiffness of some components in the machine tool-tool-workpiece system. If the vibrations are excessive, the machine stability is negatively affected. In this paper a parallel kinematic machine is modelled and structurally analyzed, considering vibrational parameters (mass, inertia, stiffness, and damping). Theoretical results are used to verify the model. The proposed model provides an effective guide to design milling machines with the best structural arrangement (architecture) and enhancing performance. The value of this finding is in answering the research question: "Should the machine tool-tool-workpiece system be kept decoupled to mitigate the vibration generated during a cutting operation?" Two approaches were proposed to determine which option (coupled or decoupled bases) provides greater dynamic rigidity. The evidence shows that the decoupled base proposal maintains a cutting operation without displacement peaks due to greater operation times and better damping response.

**Keywords:** Cutting force, dynamic stiffness, natural frequency, parallel kinematic machine, vibration analysis.

### Resumen

El fresado es una operación de corte intrínsecamente interrumpida, por tanto, se producen vibraciones. Aparecen vibraciones tanto autoexcitadas como forzadas. Las vibraciones en el fresado aparecen debido a la falta de rigidez dinámica de algunos componentes en el sistema máquina herramienta-herramienta-pieza de trabajo. Si las vibraciones son excesivas, la estabilidad de la máquina se ve afectada negativamente. En este trabajo se modela y analiza estructuralmente una máquina cinemática paralela, considerando parámetros vibratorios (masa, inercia, rigidez y amortiguación). Los resultados teóricos se utilizan para verificar el modelo. El modelo propuesto proporciona una guía eficaz para diseñar fresadoras con la mejor disposición estructural (arquitectura) y rendimiento mejorado. El valor de este hallazgo radica en responder a la pregunta de investigación: "¿Debe mantenerse desacoplado el sistema máquina herramienta-herramienta-pieza de trabajo para mitigar la vibración generada durante una operación de corte?". Se propusieron dos enfoques para determinar qué opción (bases acopladas o desacopladas) proporciona una mayor rigidez dinámica. La evidencia muestra que la propuesta de base desacoplada mantiene una operación de corte sin picos de desplazamiento debido a mayores tiempos de operación y mejor respuesta de amortiguamiento.

**Descriptores:** Análisis vibratorio, frecuencia natural, fuerzas de corte, máquina herramienta, mecanismo paralelo espacial, rigidez dinámica.

## INTRODUCTION

Parallel mechanisms for machining tasks have a special attraction for many researchers due to the design challenges involved. Manufacturers and designers of these machine tools have long maintained that one of the inherent characteristics of the parallel mechanism is their potential improved stiffness, reduced moving mass, and high dynamic performance (Enikeev *et al.*, 2018; Rosyid *et al.*, 2020; Shen *et al.*, 2020; Zhang, 2010). However, vibration induced via the excitation of structural modes can cause waviness errors and harm the machine parts resulting in errors in the workpiece surface. Finding an accurate dynamic behavior of parallel kinematic machine structures is still an intricate work (Munoa *et al.*, 2016). However, some advanced methods have been accomplished in the development of experimental methods for determination of the mode shapes of parallel kinematic machine structures. Several researchers have studied the vibration analysis of parallel kinematic machines (Mahboubkhah *et al.*, 2018; Najafi *et al.*, 2016; Yu *et al.*, 2020).

However, in most proposals, the results of modal analysis are rarely used to give a practical approach to the machine tools operators. These results are usually verified via Finite Element Modeling (FEM). Some approaches have been proposed to verify the analytical models (Chen *et al.*, 2016), to study vibrational modes of natural frequencies (Ding *et al.*, 2020; Tuffaha *et al.*, 2019), or to extract natural frequencies and mode shapes (Gao & Altintas, 2020; Gibbons *et al.*, 2020). Determining vibration characteristics of machine tools structure is of special concern in determining suitable working conditions and selecting the appropriate machining parameters to avoid self-excited vibrations in machining time.

Since modal analysis provides important information on the dynamic behavior of engineering structures, it is used as an appropriate tool to study and solve complex vibration issues on machine tools. In our approach, accurate computer simulations of machine tools structure using finite element software will lead to natural frequencies and vibration modes shapes for machine tool structure arrays. We designed structural machine tools that provide rigid support on which various subassemblies can be mounted and move the work piece and tool. These changes in the structural configuration will probably alter the natural frequencies and vibration modes of the machine. Thus, prediction and prevention of the vibration is possible in the machine tool structure for a wide range of changes in the array of these configuration (Mahboubkhah *et al.*, 2017; 2008;

2009; Pedrammehr *et al.*, 2019). In order to support the work piece and position it correctly with respect to the cutter under the influence of cutting forces, it is necessary for the structure to have high dynamic stiffness values. Two approaches are proposed to determine which variant provides greater rigidity dynamic. The proposals consist of keeping away (decoupled) or keeping together (coupled) the base that supports the workpiece and the base of the tool and the spindle/tool-holder.

The current paper is focused on the dynamic properties of a 3 degree of freedom (DoF) translational parallel kinematic machine at its resonance frequencies. These properties are identified via the FEM analysis. A model of the 3 DoF PKM is prepared in NX software. A modal analysis is applied to extract the natural frequencies and mode shape of the structure. Thus, the vibration model of a parallel kinematic machine has been presented, and relevant explicit equations are derived. Here, mass, inertia, stiffness, and damping of various elements comprising the mechanism are all considered.

## THEORETICAL DEVELOPMENT

### INTRODUCING THE 3 DOF PARALLEL KINEMATIC MACHINE

The three-prismatic-revolute-revolute-revolute (3-PRRR) configuration is a parallel mechanism with three legs, each being a 4 DoF serial mechanism (Gosselin & Kong, 2004a) (Figure 1).

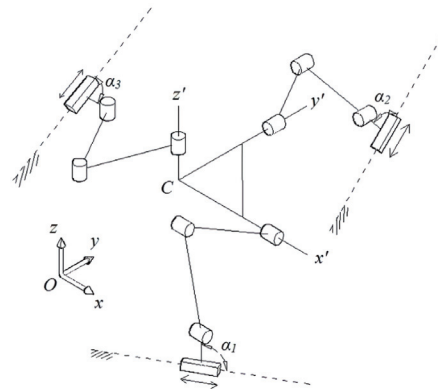


Figure 1. Schematic of the 3PRRR TPM

Each leg constrains two rotations. Therefore, the 3-PRRR configuration is an over-constrained mechanism. The terminal revolute joints of the three legs are connected to the mobile platform such that their axes are orthogonal. The most influential design parameters of the 3-PRRR are angles  $\alpha_1$ ,  $\alpha_2$ , and  $\alpha_3$  (Gosselin *et al.*,

2004b). These angles determine the output resolution as well as the overall shape of the mechanism. The three resolutions are equal when  $\alpha_1 = \alpha_2 = \alpha_3$  as well as the elements of the diagonal Jacobian matrix; the resulting mechanism is assumed to be isotropic (Zanganeh & Angeles, 1997). Moreover, the mechanism behaves exactly as a serial Cartesian mechanism when  $\alpha_1 = \alpha_2 = \alpha_3 = 0$  (X-Y-Z stage) (Gosselin *et al.*, 2004b).

#### ASSEMBLY MODE OF THE MACHINE

The forward kinematic of the 3-PRRR PKM yields an eight-degree polynomial in  $p_x$  (Kim & Tsai, 2003). Therefore, it is possible to build eight different assembly modes from the same mechanism. The Z actuator can be located anywhere perpendicular to the X-Y plane. The limbs that connect the moving platform and the XYZ actuators could have the “elbow” facing either up or down. Figure 2 shows the practical assembly mode proposed in the present work.

#### COUPLED AND DECOUPLED BASE PROPOSALS

Two approaches are proposed to determine which variant provides greater dynamic rigidity:

*Proposal 1:* Keep the base that supports the fixed workpiece to the tool's base (Figure 3a).

*Proposal 2:* Detach the base that supports the fixed workpiece from the tool's base (Figure 3b).

#### VIBRATING MODELING AND RESOLUTION OF THE MOTION EQUATIONS

The vibrating model for all the proposals was obtained from grouping the PKM's components considering them as groups of mass elements with an associated stiffness and damping capacity. Thereafter, we shall derive the governing equations of motion for each subsystem via the force-balance method.

To obtain the governing equations of motion, we use the generalized coordinate  $x$  measured from the system's static equilibrium position. Gravity forces are not considered below since the coordinates are measured from the static equilibrium position.

The parallel kinematic machine is described via inertial elements,  $m$ , along with discrete spring elements,  $k$ , and damper elements,  $c$ . All inertial elements translate only along the  $i$  direction. The external force  $F_c(t)$  in the  $i$  direction is a representative disturbance acting on the tool due to the uncut material. The free-body diagrams are used to apply the force-balance method to each inertial element.

#### MODELING METHOD AND FEM MODAL ANALYSIS

##### COUPLED BASE PROPOSAL: ONE DEGREE OF FREEDOM SYSTEM

The decoupled base proposal with one degree of freedom (DoF) is the starting point for all other cases since some values from this case are used in the other ones. This model encompasses the workpiece and its base in just one mass-spring-damper subsystem. Another subsystem encompasses the machine structure, the tool, and the toolholder. The cutting force is modeled in the contact zone between the cutter and workpiece during the cut (Figure 4).

Figure 4 assigns elements by colors to the vibrating model. Yellow-colored components correspond to  $m_1$ ,  $k_1$ , and  $c_1$ , while the blue-colored ones correspond to  $m_2$ ,  $k_2$ , and  $c_2$ . This model has only 1 DoF, and this is obtained by assuming that the tool displacement ( $x_1$ ) will be equal to that of the workpiece ( $x_2$ ), and assuming that the tool and the workpiece will be always keep in contact during the cutting process.

The motion equation for the system is:

$$\ddot{x}_1(m_1 + m_2) + \dot{x}_1(c_1 + c_2) + x_1(k_1 + k_2) = F_c \quad (1)$$

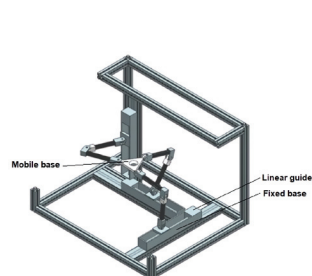


Figure 2. Design of the PKM

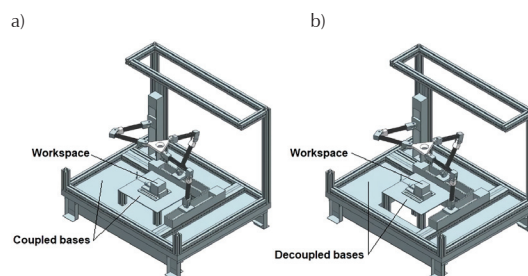


Figure 3. a) Coupled bases and b) decoupled bases of the PKM

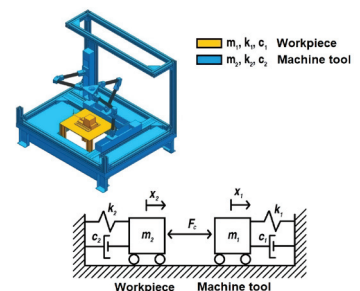


Figure 4. PKM's vibrating model with 1 DoF. Coupled base

#### COUPLED BASE PROPOSAL: TWO DEGREES OF FREEDOM SYSTEM

The coupled base proposal separately encompasses the elements that conform to the structure of the tool, the workpiece, and the base by considering that the first two are not directly connected to the ground, but are rather fixed to a common base, which is concurrently connected to the ground (Figure 5).

Figure 5 assigns elements by color to the vibrating model: Blue-colored components correspond to elements  $m_1$ ,  $k_1$ , and  $c_1$ ; yellow-colored ones correspond to  $m_2$ ,  $k_2$ , and  $c_2$ ; and gray ones correspond to  $m_3$ ,  $k_3$ , and  $c_3$ .

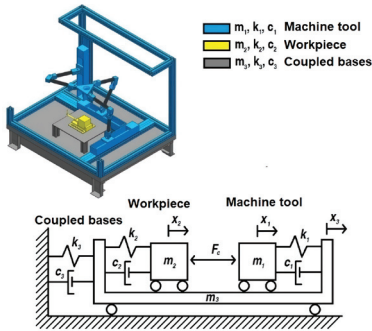


Figure 5. PKM's vibrating model with 2 DoF

Three mass-spring-damper systems can be observed in which two masses ( $m_1$  and  $m_2$ ) are joined to the same base ( $m_3$ ). By considering the displacement equality between the workpiece and the tool ( $x_1 = x_2$ ), because of the cutting force connection between them (Figure 5), a two degree of freedom system is in place with these 2 DoF being described by  $x_1$  and  $x_3$ .

The motion equations for the system are:

$$\ddot{x}_1(m_1 + m_2) + \ddot{x}_3(m_1 + m_2) + \dot{x}_1(c_1 + c_2) + \dot{x}_3(-c_1 - c_2) + x_1(k_1 + k_2) + x_3(-k_1 - k_2) = F_c \quad (2)$$

$$\ddot{x}_1(m_1 + m_2) + \ddot{x}_3(m_1 + m_2 + m_3) + \dot{x}_1(-c_1 - c_2) + \dot{x}_3(c_1 + c_2 + c_3) + x_1(-k_1 - k_2) + x_3(k_1 + k_2 + k_3) = 0 \quad (3)$$

with an equivalent representation in matrix form:

$$\begin{pmatrix} m_1 + m_2 & m_1 + m_2 \\ m_1 + m_2 & m_1 + m_2 + m_3 \end{pmatrix} \begin{pmatrix} \ddot{x}_1 \\ \ddot{x}_3 \end{pmatrix} + \begin{pmatrix} c_1 + c_2 & -c_1 - c_2 \\ -c_1 - c_2 & c_1 + c_2 + c_3 \end{pmatrix} \begin{pmatrix} \dot{x}_1 \\ \dot{x}_3 \end{pmatrix} + \begin{pmatrix} k_1 + k_2 & -k_1 - k_2 \\ -k_1 - k_2 & k_1 + k_2 + k_3 \end{pmatrix} \begin{pmatrix} x_1 \\ x_3 \end{pmatrix} = \begin{pmatrix} F_c \\ 0 \end{pmatrix} \quad (4)$$

Or:

$$\mathbb{M}\ddot{\mathbb{X}} + \mathbb{C}\dot{\mathbb{X}} + \mathbb{K}\mathbb{X} = \mathbb{F} \quad (5)$$

Here  $\mathbb{M}$ ,  $\mathbb{C}$ ,  $\mathbb{K}$ ,  $\ddot{\mathbb{X}}$ ,  $\dot{\mathbb{X}}$ ,  $\mathbb{X}$  and  $\mathbb{F}$  are the matrix for mass, damping, stiffness, acceleration, velocity, displacement, and force, respectively.

$$\mathbb{M} = \begin{pmatrix} m_1 + m_2 & m_1 + m_2 \\ m_1 + m_2 & m_1 + m_2 + m_3 \end{pmatrix}$$

$$\mathbb{C} = \begin{pmatrix} c_1 + c_2 & -c_1 - c_2 \\ -c_1 - c_2 & c_1 + c_2 + c_3 \end{pmatrix}$$

$$\mathbb{K} = \begin{pmatrix} k_1 + k_2 & -k_1 - k_2 \\ -k_1 - k_2 & k_1 + k_2 + k_3 \end{pmatrix}$$

$$\mathbb{X} = \begin{pmatrix} x_1 \\ x_3 \end{pmatrix}$$

$$\dot{\mathbb{X}} = \begin{pmatrix} \dot{x}_1 \\ \dot{x}_3 \end{pmatrix}$$

$$\ddot{\mathbb{X}} = \begin{pmatrix} \ddot{x}_1 \\ \ddot{x}_3 \end{pmatrix}$$

$$\mathbb{F} = \begin{pmatrix} F_c \\ 0 \end{pmatrix}$$

#### DECOUPLED BASES PROPOSAL: THREE DEGREES OF FREEDOM SYSTEM

In this proposal, the two mass-spring-damper system in series are present: One corresponds to the tool and the other one to the workpiece.

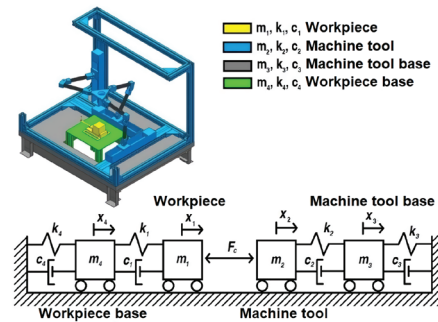


Figure 6. PKM's vibrating model with 3 DoF

Figure 6 assigns elements by color to the vibrating model. Yellow components correspond to elements  $m_1$ ,  $k_1$ , and  $c_1$ ; blue ones correspond to  $m_2$ ,  $k_2$ , and  $c_2$ ; gray ones correspond to  $m_3$ ,  $k_3$ , and  $c_3$ ; green-colored ones correspond to  $m_4$ ,  $k_4$ , and  $c_4$ .



pond to  $m_4$ ,  $k_4$  and  $c_4$ . In this vibrating model, a total of four mass-spring-damper systems are present and grouped by pairs. Mass pairs are connected via the cutting force similar to the two degrees of freedom system; therefore,  $x_1$  equals  $x_2$  for a total of three degrees of freedom described as  $x_1$ ,  $x_3$  and  $x_4$ .

The motion equations for the system are:

$$\begin{pmatrix} m_1 + m_2 + m_3 & m_3 & m_1 + m_2 + m_3 \\ m_3 & m_3 & m_3 \\ m_1 + m_2 + m_3 & m_3 & m_1 + m_2 + m_3 + m_4 \end{pmatrix} \begin{pmatrix} \ddot{x}_1 \\ \ddot{x}_3 \\ \ddot{x}_4 \end{pmatrix} +$$

(6)

$$\begin{pmatrix} c_1 + c_2 & -c_2 & -c_1 \\ -c_2 & c_2 + c_3 & 0 \\ -c_1 & 0 & c_1 + c_4 \end{pmatrix} \begin{pmatrix} \dot{x}_1 \\ \dot{x}_3 \\ \dot{x}_4 \end{pmatrix} + \begin{pmatrix} k_1 + k_2 & -k_2 & -k_1 \\ -k_2 & k_2 + k_3 & 0 \\ -k_1 & 0 & k_1 + k_4 \end{pmatrix} \begin{pmatrix} x_1 \\ x_3 \\ x_4 \end{pmatrix} = \begin{pmatrix} F_c \\ 0 \\ 0 \end{pmatrix}$$

Or:

$$\mathbb{M}\ddot{\mathbb{X}} + \mathbb{C}\dot{\mathbb{X}} + \mathbb{K}\mathbb{X} = \mathbb{F} \quad (7)$$

Here  $\mathbb{M}$ ,  $\mathbb{C}$ ,  $\mathbb{K}$ ,  $\ddot{\mathbb{X}}$ ,  $\dot{\mathbb{X}}$ ,  $\mathbb{X}$  and  $\mathbb{F}$  are the matrix for mass, damping, stiffness, acceleration, velocity, displacement, and force, respectively.

$$\mathbb{M} = \begin{pmatrix} m_1 + m_2 + m_3 & m_3 & m_1 + m_2 + m_3 \\ m_3 & m_3 & m_3 \\ m_1 + m_2 + m_3 & m_3 & m_1 + m_2 + m_3 + m_4 \end{pmatrix}$$

$$\mathbb{C} = \begin{pmatrix} c_1 + c_2 & -c_2 & -c_1 \\ -c_2 & c_2 + c_3 & 0 \\ -c_1 & 0 & c_1 + c_4 \end{pmatrix}$$

$$\mathbb{K} = \begin{pmatrix} k_1 + k_2 & -k_2 & -k_1 \\ -k_2 & k_2 + k_3 & 0 \\ -k_1 & 0 & k_1 + k_4 \end{pmatrix}$$

$$\mathbb{X} = \begin{pmatrix} x_1 \\ x_3 \\ x_4 \end{pmatrix}$$

$$\dot{\mathbb{X}} = \begin{pmatrix} \dot{x}_1 \\ \dot{x}_3 \\ \dot{x}_4 \end{pmatrix}$$

$$\ddot{\mathbb{X}} = \begin{pmatrix} \ddot{x}_1 \\ \ddot{x}_3 \\ \ddot{x}_4 \end{pmatrix}$$

$$\mathbb{F} = \begin{pmatrix} F_c \\ 0 \\ 0 \end{pmatrix}$$

## OBTAINING MODAL PARAMETERS AND RESOLVING MOTION EQUATIONS

Mass is obtained by employing NX software via the materials shown in Table 1. This leads to the magnitudes shown in Table 2.

Table 1. Materials of the solid model in NX

Subsystem	Component	Material
Workpiece	Legs (profiles)	Aluminum 6061
	Table	Steel
	Workpiece holder	Steel
	Workpiece	Steel
Tool	Machine structure (profiles)	Aluminum 6061
	Linear guides	Steel
	Joints	ABS
	Links	Aluminum 6061
	Table	Brass

Table 2. Mass values

System	Mass	Magnitude [kg]
1 DoF	$m_1$	305.1013
	$m_2$	11.8083
2 DoF	$m_1$	50.208
	$m_2$	4.2585
	$m_3$	302.3477
3 DoF	$m_1$	4.2585
	$m_2$	50.2080
	$m_3$	254.8933
	$m_4$	7.5490

The concept of natural frequency relates mass to stiffness. By already knowing the value of each of the model's masses, it is only matter of finding the natural frequency value associated with each mass-spring-damper system. This value was obtained via FEM. The mesh parameters used for the simulation are shown in Table 3.

Subsequently, the concept of critic damping is employed for a 1 DoF mass-spring-damper system, assuming an underdamped operation with a damping factor of 0.5.

The subsystems from the 1 DoF case are the simplification of the subsystems from the 3 DoF case. Thus, the stiffness constant and equivalent damping were employed to obtain the stiffness and damping values of the 3 DoF model as well as the supposition where  $k_1 > k_4$ ,  $k_3 > k_2$ ,  $c_1 > c_4$  and  $c_3 > c_2$ . These values are based on the discrepancy of magnitudes of the natural frequencies obtained by finite element for each of the mass-

spring-damper subsets from the 3 DoF case (tool, spindle-toolholder, workpiece and workpiece-holder). Thus, a stiffness and damping proposal for the 3 DoF system is obtained. This proposal maintains a similar proportion to the values of natural frequency associated with each subset.

Finally, the mass, stiffness and damping values corresponding to the subsystems supported by the bases were set equal between these 2 DoF and 3 DoF systems because the difference between the 3 DoF and 2 DoF systems comes down to the bases (the systems above these are the same). However, since the 2 DoF system's base shows a remarkable geometric similarity with the 3 DoF system's tool base, the mass values, stiffness, and damping values were set equal. The stiffness and damping values associated with each model are shown on Table 4.

#### CUTTING FORCE

Machining conditions that produce discontinuous chips cause variations of the cutting forces. Therefore, the stiffness of the cutting tool holder and the machine tool is of major importance in avoiding vibrations that

deteriorate the surface finish. During milling, the process of cutting by each tooth is periodically interrupted and the traverse cross section of the undeformed chip is variable (El-Hofy, 2014). Thus, by assuming a face milling operation, a nonsymmetrical bilateral case of an entrance angle  $\phi_1$ , and leaving angle  $\phi_2$ , the chip mean thickness can be calculated on a single tooth from the equation:

$$F_m = k_s b h_{m(x)} \quad (8)$$

where  $k_s$  is the cutting stiffness, and  $b h_{m(x)}$  is the area of cutting contact with a tool setting angle of  $\alpha = 90^\circ$ . The total mean force in the direction of cutting speed  $V$  becomes

$$F_t = \frac{k_s f_z h Z_c [\cos(\phi_1) - \cos(\phi_2)]}{2\pi} \quad (9)$$

where  $f_z$  is the feed per tooth and  $Z_c$  is the number of teeth.

Table 5 summarizes the cutting parameters considering some middle power cutting parameters according to Table 2.4 in (Isakov, 2003).

Table 3. Mesh parameters

Subsystem	Elements size [mm]	Component	Bodies	Material
Workpiece	10	Legs (profiles)	4	Aluminum 6061
	10	Table	1	Steel
	10	Workpiece holder	2	Steel
	10	Workpiece	1	Steel
	10	Machine structure (profiles)	16	Aluminum 6061
Tool	15	Linear guides	3	Steel
	10	Joints	16	ABS
	5	Links	6	Aluminum 6061
	15	Table	1	Brass
	10	Legs (profiles)	8	Steel

Table 4. Stiffness and damping values

System	Stiffness	Magnitude [N/ $\mu$ m]	Damping	Magnitude [N·s/m]
1 DoF	$k_1$	0.183945	$c_1$	0.007941
	$k_2$	0.177989	$c_2$	0.001449
2 DoF	$k_1$	0.258531	$c_1$	0.010528
	$k_2$	1.049272	$c_2$	0.008542
	$k_3$	0.637595	$c_3$	0.025965
3 DoF	$k_1$	1.049272	$c_1$	0.008542
	$k_2$	0.258531	$c_2$	0.010528
	$k_3$	0.637595	$c_3$	0.025965
	$k_4$	0.214349	$c_4$	0.001745

Table 5. Cutting parameters estimated for the PKM

$k_s = 2059.4 \text{ [N/mm}^2\text{]}$	$h = 3.81 \text{ [mm]}$	$fz = 0.2032 \text{ [mm]}$
$Z_c = 4 \text{ [teeth]}$	$\varphi_1 = 45^\circ$	$\varphi_2 = 135^\circ$

#### MOTION EQUATIONS RESOLUTION

The motion equations for the vibrating models were obtained via the Euler method for differential equations defining position and velocity in function of velocity and acceleration, respectively, associated with a step size  $h_p$ . A big step size can lead to a wrong approximation in the direct mathematic outcome. On the other hand, a small step size offers a better approximation although it requires more time for its resolution. One way to establish an appropriate step size within mechanical systems is to make a phase space graph with displacement and velocity as variables.

The lack of dissipation elements in a vibrating system causes a cyclic response that does not allow reduction in neither displacements nor velocities. This generates closed curves in displacement versus velocities graphs. This phenomenon is useful to define the adequate step size for the differential equations to solve. By evaluating many step size values, we found that  $h_p=0.001$  is sufficient, since this value already reflects the cyclic behavior of the displacements and velocities of a 1 DoF vibrating system with no dissipation elements present.

The resolution of the previously mentioned equations was developed by employing Euler's method for differential equations by starting off from initial values ( $t = 0 \text{ s}$ ) with a  $0.1 \text{ }\mu\text{m}$  value for each one of the displacements ( $x_1, x_2, x_3$ , etc.) and a  $0 \text{ }\mu\text{m/s}$  value for each velocity ( $v_1, v_2, v_3$ , etc.). Furthermore, gathering the mass, damping, stiffness, and natural frequencies values was supported by finite element simulation with NX Software and making use of NX Nastran solver with a structural type analysis using "SOL 103 Response Simulation" solve tool.

#### NUMERICAL METHOD FOR THE 2 DOF MODEL (COUPLED BASE)

We next employed the Euler method for resolution of differential equations:

$$\mathbb{X}_{i+1} = \mathbb{X}_i + h\dot{\mathbb{X}}_i \quad (10)$$

$$\ddot{\mathbb{X}} = \mathbb{M}^{-1}\mathbb{F} - \mathbb{M}^{-1}\mathbb{C}\dot{\mathbb{X}} - \mathbb{M}^{-1}\mathbb{K}\mathbb{X} \quad (11)$$

$$\dot{\mathbb{X}}_{i+1} = \dot{\mathbb{X}}_i + h * (\mathbb{M}^{-1}\mathbb{F} - \mathbb{M}^{-1}\mathbb{C}\dot{\mathbb{X}} - \mathbb{M}^{-1}\mathbb{K}\mathbb{X}) \quad (12)$$

Where:

$$\mathbb{X}_i = \begin{pmatrix} x_{1 \rightarrow i} \\ x_{3 \rightarrow i} \end{pmatrix}$$

$$\mathbb{X}_{i+1} = \begin{pmatrix} x_{1 \rightarrow i+1} \\ x_{3 \rightarrow i+1} \end{pmatrix}$$

$$\dot{\mathbb{X}}_i = \begin{pmatrix} \dot{x}_{1 \rightarrow i} \\ \dot{x}_{3 \rightarrow i} \end{pmatrix}$$

$$\dot{\mathbb{X}}_{i+1} = \begin{pmatrix} \dot{x}_{1 \rightarrow i+1} \\ \dot{x}_{3 \rightarrow i+1} \end{pmatrix}$$

$$\mathbb{M}^{-1} = \frac{1}{m_1 m_3 + m_2 m_3} \begin{pmatrix} m_1 + m_2 + m_3 & -m_1 - m_2 \\ -m_1 - m_2 & m_1 + m_2 \end{pmatrix}$$

Being  $x_{1 \rightarrow i}$  and  $\dot{x}_{1 \rightarrow i}$  the displacements and velocities, respectively. These correspond to the  $i$ -iteration for the  $x_1$  variable, while  $x_{1 \rightarrow i+1}$  and  $\dot{x}_{1 \rightarrow i+1}$  correspond to the displacements and velocities, respectively, inherent to the  $x_1$  variable at the subsequent iteration.

#### NUMERICAL METHOD FOR THE 3 DOF MODEL (DECOUPLED BASES)

We next employed the Euler method for differential equations resolution:

$$\ddot{\mathbb{X}} = \mathbb{M}^{-1}\mathbb{F} - \mathbb{M}^{-1}\mathbb{C}\dot{\mathbb{X}} - \mathbb{M}^{-1}\mathbb{K}\mathbb{X} \quad (13)$$

$$\dot{\mathbb{X}}_{i+1} = \dot{\mathbb{X}}_i + h * (\mathbb{M}^{-1}\mathbb{F} - \mathbb{M}^{-1}\mathbb{C}\dot{\mathbb{X}} - \mathbb{M}^{-1}\mathbb{K}\mathbb{X}) \quad (14)$$

While, for the displacement matrix:

$$\mathbb{X}_{i+1} = \mathbb{X}_i + h\dot{\mathbb{X}}_i \quad (15)$$

Where:

$$\mathbb{X}_i = \begin{pmatrix} x_{1 \rightarrow i} \\ x_{3 \rightarrow i} \\ x_{4 \rightarrow i} \end{pmatrix}$$

$$\mathbb{X}_{i+1} = \begin{pmatrix} x_{1 \rightarrow i+1} \\ x_{3 \rightarrow i+1} \\ x_{4 \rightarrow i+1} \end{pmatrix}$$

$$\dot{\mathbb{X}}_i = \begin{pmatrix} \dot{x}_{1 \rightarrow i} \\ \dot{x}_{3 \rightarrow i} \\ \dot{x}_{4 \rightarrow i} \end{pmatrix}$$



$$\dot{\mathbf{x}}_{i+1} = \begin{pmatrix} \dot{x}_{1 \rightarrow i+1} \\ \dot{x}_{3 \rightarrow i+1} \\ \dot{x}_{4 \rightarrow i+1} \end{pmatrix}$$

$$\mathbb{M}^{-1} = \frac{1}{M} \begin{pmatrix} m_1 m_3 + m_2 m_3 + m_3 m_4 & -m_3 m_4 & -m_1 m_3 - m_2 m_3 \\ -m_3 m_4 & m_1 m_4 + m_2 m_4 + m_3 m_4 & 0 \\ -m_1 m_3 - m_2 m_3 & 0 & m_1 m_3 + m_2 m_3 \end{pmatrix}$$

With:

$$M = m_1 m_3 m_4 + m_2 m_3 m_4$$

## RESULTS

The results were obtained using equations (9) and (11) for the 2 DoF system, and equations (12) and (13) for the 3 DoF one. Figure 7 shows displacements for  $x_1$ ,  $x_3$ , and  $x_4$  within the initial 200 s of the milling operation. The maximum values are close to 7000  $\mu\text{m}$  with a significant difference for  $x_3$ . Figure 8 shows the displacement response along 1000 s. This behavior has a period of 400 s.

Figure 9 shows the behavior of velocities  $v_1$ ,  $v_3$ , and  $v_4$  along 200 s. The maximum values are close to 300  $\mu\text{m/s}$  with a significant difference in magnitude for  $v_3$ . The  $v_3$  maximum values match with  $v_4$  minimum values

on each cycle. Figure 10 shows the velocity behavior previously mentioned along 1000 s, which allows observation of the stabilization that occurs progressively except for  $v_3$ , which seems to maintain the same behavior and magnitudes throughout.

Figure 11 shows the displacement behavior of  $x_1$  and  $x_3$  along 200 s. These have the maximum values around 6000  $\mu\text{m/s}$  and 5000  $\mu\text{m/s}$ , respectively. Figure 12 shows the displacement behavior of  $x_1$  and  $x_3$  along 1000 s. This behavior has a period of 180 s.

Figure 13 shows velocities  $v_1$  and  $v_3$  along 200 s with maximum magnitudes close to  $\pm 200$   $\mu\text{m/s}$  for  $v_1$ , while  $v_2$  shows maximum values of half that magnitude. Figure 14 shows velocities  $v_1$  and  $v_3$  along 1000 s with a period of approximately 180 s. In this case, the velocities do not have significant damping.

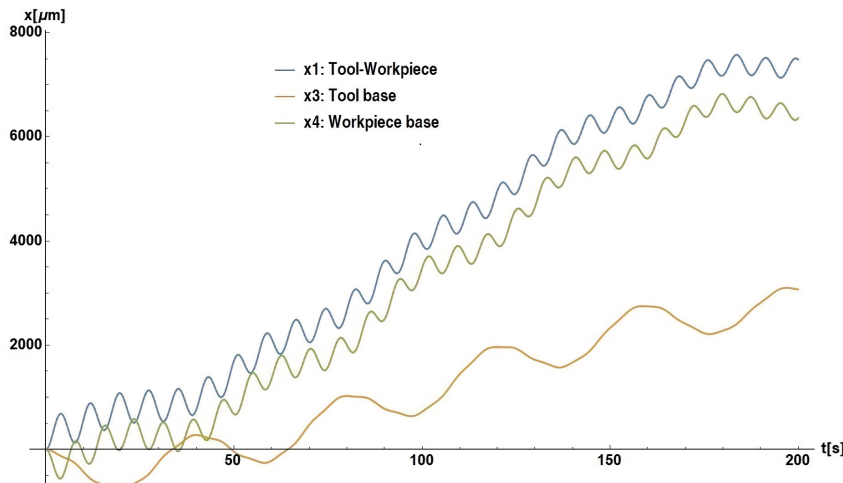


Figure 7. Displacement of the 3 DoF system (decoupled bases) 200 [s]

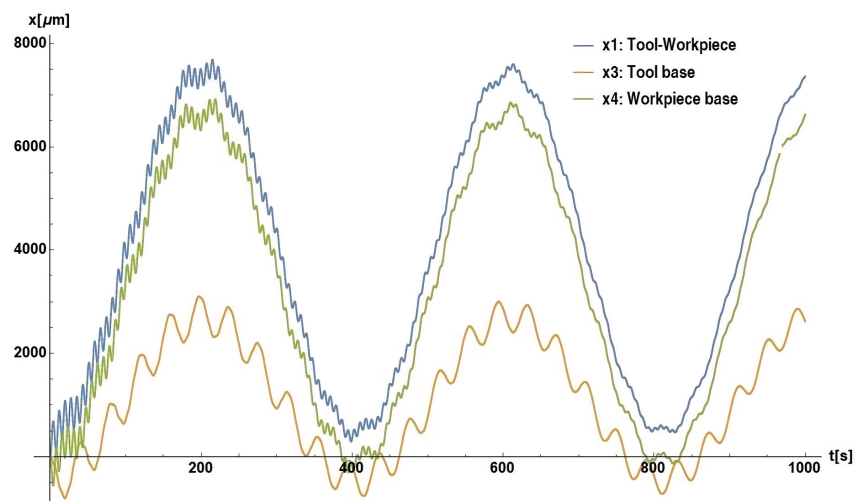


Figure 8. Displacement of the 3 DoF system (decoupled bases) 1000 [s]

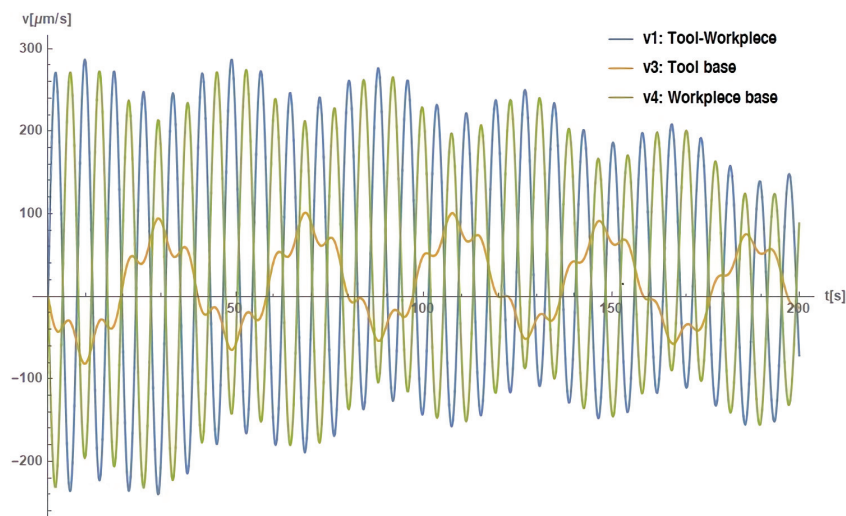


Figure 9. Velocities of the 3 DoF system (decoupled bases) 200 [s]

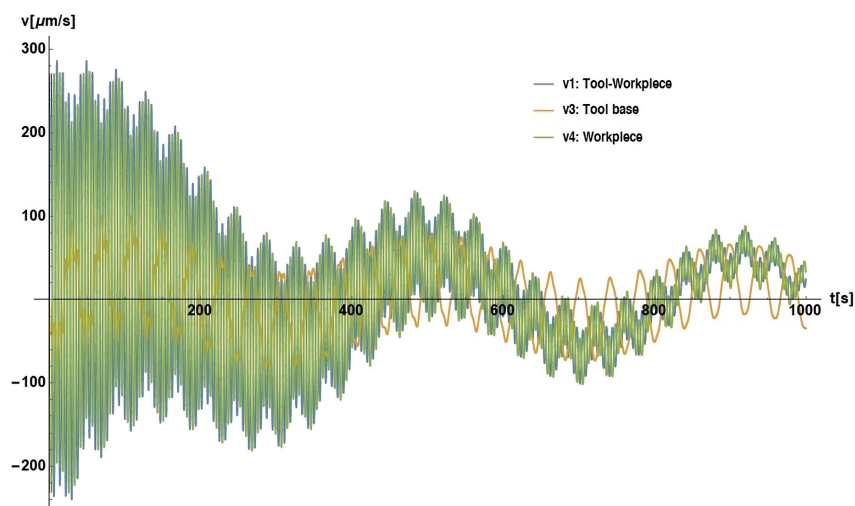


Figure 10. Velocities of the 3 DoF system (decoupled bases) 1000 [s]

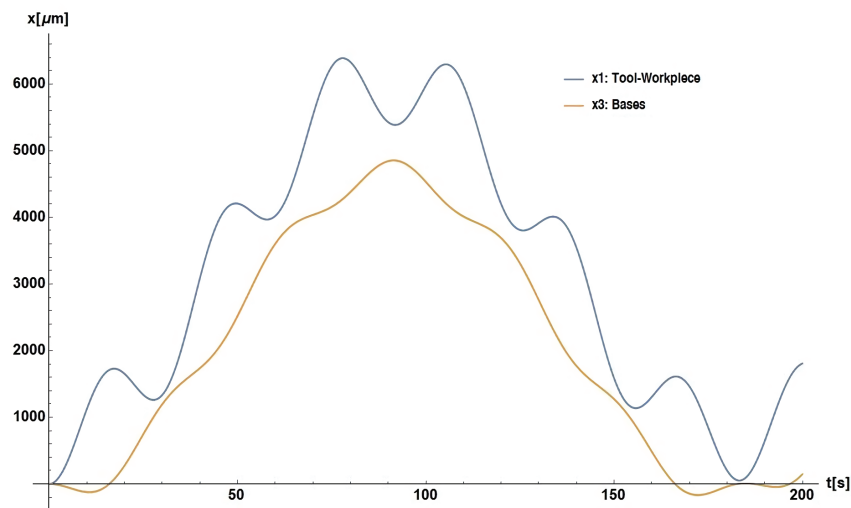


Figure 11. Displacement of the 2 DoF system (coupled bases) 200 [s]

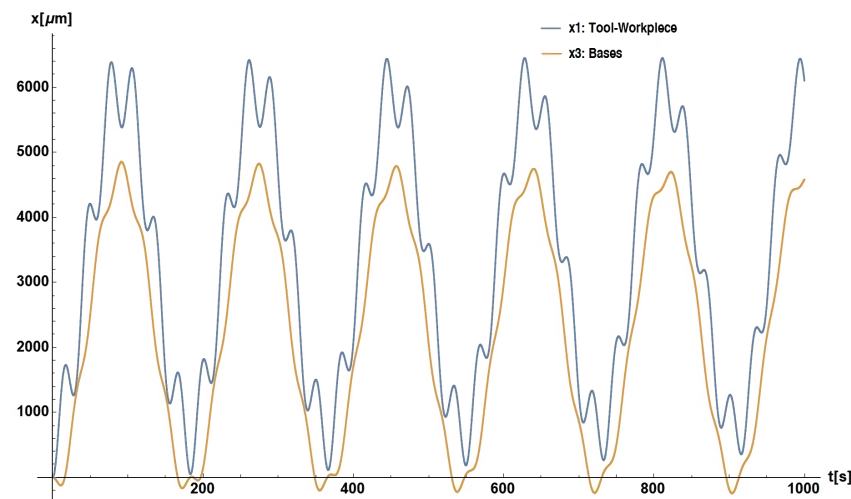


Figure 12. Displacement of the 2 DoF system (coupled bases) 1000 [s]

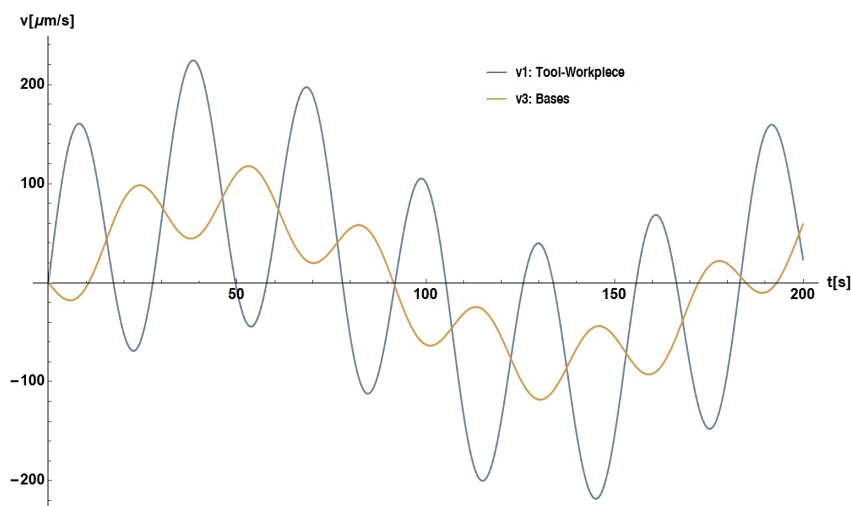


Figure 13. Velocities of the 2 DoF system (coupled bases) 200 [s]

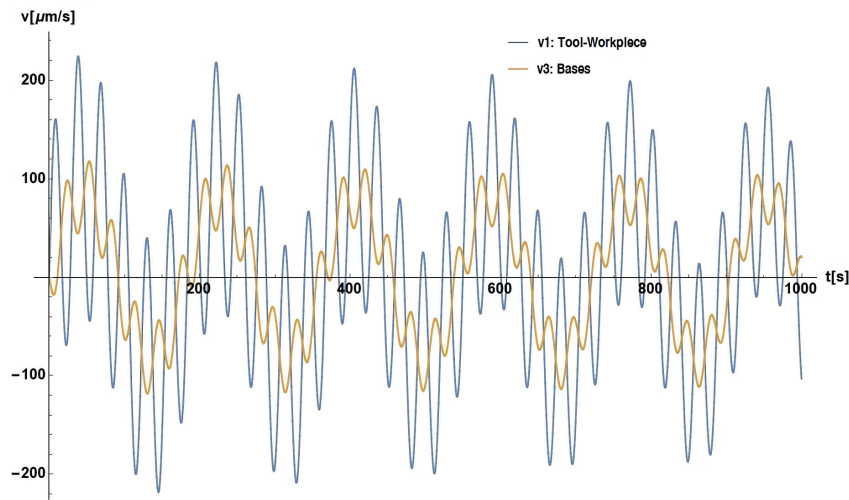


Figure 14. Velocities of the 2 DoF system (coupled bases) 1000 [s]

## DISCUSSION

In the first instance, the maximum values for displacement and velocity from the 2 DoF system are lower than those for the 3 DoF system. Nevertheless, that fact does not necessarily mean that it is better; the maximum displacements and velocities correspond to the variable associated with the interaction between the tool and workpiece subsystems. The values oscillate between 7600 [ $\mu\text{m}$ ] and 280 [ $\mu\text{m/s}$ ] in the decoupled bases, while in the coupled base proposal, these values oscillate between 6400 [ $\mu\text{m}$ ] and 220 [ $\mu\text{m/s}$ ], which is 1.57 % less for displacements and 21 % for velocities both with respect to the 3 DoF system.

On the other hand, the general behavior of the displacements in the 3 DoF system is repeated in longer periods (every 400 seconds, approximately), but it is repeated in shorter periods (every 200 seconds, approximately) in the 2 DoF system. This can be interpreted as behaviors with smaller frequencies for this first system, and greater ones for the second one. This means that the decoupled base proposal will reach its maximum displacements in a longer period compared to the coupled base proposal. Therefore, these values for maximum displacements in the 3 DoF system will be prevented more easily via constant cutting times below 200 seconds.

The 3 DoF system has an overall better damping than the 2 DoF one; hence, displacements at lower velocities can be expected as the cutting process advances through time in this first system. In the second system, velocities do not achieve a significant reduction in value. Nonetheless, by considering the factors mentioned in the previous paragraph (cutting operations below

200 seconds), a substantial reduction in velocities could not happen because the first major velocity reduction does not appear until 320 seconds. The velocities are 44 % lower than the initial ones.

The decoupled base proposal shows an overall better performance under these considerations. A simplified solid model of the proposal can be observed in Figure 15.

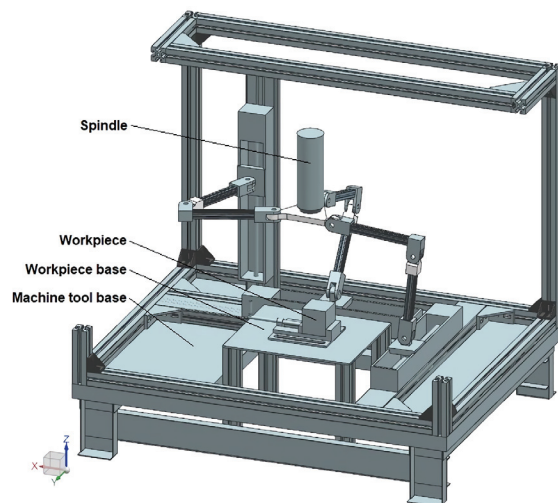


Figure 15. Final design (decoupled bases approach)

The results for the displacements and velocities in both design proposals are too large for machining with industrial standards. Nevertheless, this can be broadened to the PKM modeling because this only represents the two inertial elements instead of making a model that englobes each component of the real system as an additional inertial element. This great scale response can be

translated as the sum of displacements associated with diverse components of each subsystem. This is only for the displacements present in the real interaction between tool and workpiece.

Furthermore, the validity of the natural frequency values obtained via simulation for the different elements of the solid models was evaluated by making theoretical calculations of the natural frequency for a rod-type structure without any support (made out of steel with square cross-section with 20 [mm] per side and a length of 400 [mm] as well as  $\rho=7829$  [kg/m<sup>3</sup>] and  $E=206.94$  [GPa]). We then compared theoretical values with the ones obtained by the simulation. We compared the lower value of natural frequency associated with each natural vibration mode to obtain the results shown in Table 6.

Table 6. Error associated with the natural frequency calculations via simulation

Mode	$f_{sim}$ [Hz]	$f_{analyt}$ [Hz]	Error [%]
1	654	661	1.11
2	1774	1821	2.62
3	3400	3571	4.83
4	5465	5903	7.45
5	7904	8826	10.47

Table 6 shows the values obtained by simulation ( $f_{sim}$ ) and the values obtained analytically ( $f_{analyt}$ ). The data show how the error increases alongside the normal vibration mode at issue. However, an error of approximately 1.11 % is totally acceptable because the lowest natural frequency of each assembly was always used (the one associated with the first normal vibration mode).

## CONCLUSION

This paper describes structural analysis of a 3 degree of freedom parallel kinematic machine. The theoretical results were used to demonstrate the viability of the modeling approach. The proposed model provides an effective guide to design milling machines with the best architecture and enhancing performance. Two assembly proposals were modeled and analyzed. The decoupled base design proposal has a better performance characteristic to develop machining operations. It can maintain a cutting operation without displacement peaks due to greater operation times and better damping response.

## ACKNOWLEDGES

This work was supported by UNAM-PAPIIT IN119120.

## REFERENCES

- Gosselin, C. M. & Kong, X. (2004). Cartesian Parallel Manipulators, US Patent No. 6,729,202 B2 May 4.
- Gosselin, C., Kong, X., Foucault, S. & Bonev, I. (2004). A fully-decoupled 3-DOF translational parallel mechanism. In Proc. 4th Chemnitz Parallel Kinematics Seminar (PKS), pp. 595-610.
- Chen, Z. S., Liu, M., Kong, M. X. & Ji, C. (2016). Modal analysis of high-speed parallel manipulator with flexible links. *Applied Mechanics and Materials*, 826, 8-14. <https://doi.org/10.4028/www.scientific.net/amm.826.8>
- Ding J., Chang Y., Chen P., Zhuang H., Ding Y., Lu H. & Chen Y. (2020). Dynamic modeling of ultra-precision fly cutting machine tool and the effect of ambient vibration on its tool tip response. *Int. J. Extrem. Manuf.*, 2(2), 025301. <https://doi.org/10.1088/2631-7990/ab7b59>
- El-Hofy, H.G. (2014). Fundamentals of machining processes. BoR.
- Kudoyarov (2018). Experimental Stiffness Analyses of a 3-DOF Parallel Kinematics Machine-Tool. International Russian Automation Conference (RusAutoCon), Sochi, 2018, pp. 1-4. <https://doi.org/10.1109/RUSAUTOCON.2018.8501802>
- Gao J. & Altintas Y. (2020). Chatter stability of synchronized elliptical vibration assisted milling. *CIRP Journal of Manufacturing Science and Technology*, 28, 76-86. <https://doi.org/10.1016/j.cirpj.2019.11.006>
- Gibbons T. J., Ozturk E., Xu L., Sims N. D. (2020). Chatter avoidance via structural modification of tool-holder geometry. *Int. J. Mach. Tools Manuf.*, 103514. <https://doi.org/10.1016/j.ijmachtools.2019.103514>
- Isakov, E. (2003). *Engineering Formulas for Metalcutting*: Industrial Press, Inc.
- Kim, H. S. & Tsai, L. (2003). Design optimization of a cartesian parallel manipulator. *ASME. J. Mech. Des.*, 125(1): 43-51. <https://doi.org/10.1115/1.1543977>
- Mahboubkhah, M., Pakzad, S., Ghane Arasi, A. & Etefagh, M. M. (2017). Modal analysis of the vertical moving table of 4-DOF parallel machine tool by FEM and experimental test. *Journal of Vibroengineering*, 19(7), 5301-5309. <https://doi.org/10.21595/jve.2017.18394>
- Mahboubkhah, M., Nategh, M. J. & Esmaeilzade-Khadem, S. (2008). Vibration analysis of machine tool's hexapod table. *Int J Adv Manuf Technol*, 38, 1236-1243. <https://doi.org/10.1007/s00170-007-1183-9>
- Mahboubkhah, M., Nategh, M. J. & Esmaeilzadeh-Khadem, S. (2009). A comprehensive study on the free vibration of machine tools' hexapod table. *Int J Adv Manuf Technol*, 40, 1239-1251. <https://doi.org/10.1007/s00170-008-1433-5>
- Mahboubkhah, M., Pakzad, S., Sadeghi, M. H. & Etefagh, M. M. (2018). Vibration Analysis of 2-PR(Pa)U- 2-PR(Pa)R New Parallel Mechanism. *ADMT Journal*, 10(4), 1-6.
- Munoa, J., Beudaert, X., Dombovari, Z., Altintas, Y., Budak, E., Brecher, C., Stepan, G. (2016). Chatter suppression techniques



- in metal cutting. *CIRP Annals*, 65(2), 785-808. <https://doi.org/10.1016/j.cirp.2016.06.004>
- Najafi, A., Movahhedy, M. R., Zohoor, H., Alasty, A. (2016). Dynamic stability of a Hexaglide machine tool for milling processes. *Int J Adv Manuf Technol.*, 86, 1753-1762. <https://doi.org/10.1007/s00170-015-8331-4>
- Pedrammehr, S., Asadi, H. & Nahavandi, S. (2019). The forced vibration analysis of hexarot parallel mechanisms. *IEEE International Conference on Industrial Technology (ICIT)*, 199-204. <https://doi.org/10.1109/ICIT.2019.8755207>
- Rosyid, A., El-Khasawneh, B. & Alazzam, A. (2020). Review article: Performance measures of parallel kinematics manipulators. *Mech. Sci.*, 11(1), 49-73. <https://doi.org/10.5194/ms-11-49-2020>
- Shen, N., Geng, L., Li, J., Ye, F., Yu, Z. & Wang, Z. (2020). Improved stiffness modeling for an exechon-like Parallel Kinematic Machine (PKM) and its application. *Chin. J. Mech. Eng.* 33, 40. <https://doi.org/10.1186/s10033-020-00451-5>
- Tuffaha M., Bazoune A., Al-Badour F., Merah N. & Shuaib A. (2019). Dynamic modeling and analysis of a horizontal operating 3-Axis machine for friction stir welding. *IEEE Access*, 7, 129874-129882, 2019. <https://doi.org/10.1109/ACCESS.2019.2939300>
- Yu G., Wang L., Wu J., Gao Y. (2020). Milling stability prediction of a hybrid machine tool considering low-frequency dynamic characteristics. *Mech. Syst. Sig. Process*, 135, 106364. <https://doi.org/10.1016/j.ymssp.2019.10636>
- Zanganeh, K. E. & Angeles, J. (1997). Kinematic isotropy and the optimum design of parallel manipulators. *The International Journal of Robotics Research*, 16(2), 185-197. <https://doi.org/10.1177/027836499701600205>
- Zhang, D. (2010). *Parallel robotic machine tool*. Springer-Verlag US. 1st ed. <https://doi.org/10.1007/978-1-4419-1117-9>